Evaluation of the Influence of the Nucleation Undercooling on Columnar Grain Growth During Al-Cu Alloy Directional Solidification

F. Shadfar*

School of Metallurgy and Materials Engineering, Iran University of Science and Technology, Tehran, Iran.
Received: 19 June 2018 - Accepted: 12 August 2018

Abstract

An analytical model was developed to evaluate the influence of initial grain density over the chill on the texture formation during directional solidification. The model is based on competitive grain growth mechanism. The Al - 3wt%Cu alloy was used in a directional solidification process to verify the accuracy of the model. Two different nucleation densities over the chill plate were produced using various water flow rates in the cooling system. Cooling curves of the alloy during solidification were monitored using thermal analysis. Optical microscopy and image analysis were used to analyze the grain structure of the solidified samples. Also, the cellular automaton finite element (CAFE) method was used for numerical calculations to comprise the results of the present analytical model with numerical simulation. The results showed that the increment of the nucleation undercooling would ease the formation of well-oriented <001> texture in the starter block. Experimental and numerical data were in good agreement with the results of analytical model.

Keywords: Directional Solidification, Growth Model, Nucleation, Heat Transfer

1. Introduction

Elimination of high angle grain boundaries is the most effective way to improve the creep resistance of directionally solidified gas turbine blades for high temperature applications [1-3]. On the other hand, producing <001> texture parallel to the longitudinal axis of the blade is favorable to reduce thermal fatigue as a result of lowering the elastic module in Nickel base superalloys [4]. Bridgman method is usually used to produce directionally solidified samples. It produces a uniaxial thermal gradient to encourage the columnar growth of dendrites with preferred <001> orientation in the opposite of the heat flow direction. Producing of a well-oriented structure in directionally solidified turbine blades is as a result of competitive growth mechanism. In this mechanism, well-oriented dendrites grow over the mis-oriented dendrites and so suppress their further growth [5,6].

A pigtail crystal selector is mostly used to produce single crystal turbine blades in industrial applications. It consists of two main parts; a starter block which produces a preferred <001> texture as a result of competitive growth mechanism and a spiral part which select only one grain by blocking and branching phenomena.[7-10] Performance of starter block in the production of near <001> texture is very important to produce well-aligned directionally solidified and single crystal blades. So evaluation of parameters affecting the performance of this part is important.

Many investigations have been conducted to study the mechanism of competitive growth of two neighboring dendrites using bi-crystals and/or transparent physical models [11].

In the case of a starter block, there exists many grains which take part in the competitive growth and the situation is more complicated.

Although numerical calculations using Cellular Automaton-Finite element (CAFE) and phase field simulation method are applied to predict the structural changes during directional solidification [12-15], these methods consume long time for modeling of the process.

There is few or no engineering model to describe the effective parameters on the texture formation in the starter block, specially the effect of nucleation kinetic on the chill/melt interface.

The model proposed here is an analytical model for the determination of the effect of nucleation density on texture evolution taking place during directional solidification of multicrystalline<100>dendritic structures.

The objective is justified if one needs a rapid computation or a solution to compare with numerical simulations.

Using the analytical model, one can control texture formation in directional solidification and single crystal growth process.

The results of the present model were compared with experimental data as well as the results obtained from CAFE module which frequently used for simulation of solidified structure in directional solidification process [12,14,16].

*Corresponding author
Email address: farnazshadfar2018@gmail.com

2. Materials and Methods

2.1. Description of Analytical Model

In order to evaluate the effect of nucleation kinetics on texture formation, here we describe a 2-D analytical model. During the initial stages of directional solidification using Bridgman technique, heat is mainly extracted through the water-cooled chill. Therefore, heterogeneous nucleation would be occurred on the melt/chill interface and equiaxed grains will be formed rapidly on the chill plate due to high undercooling imposed by the water-cooled chill. Columnar dendrites then rapidly grow from equiaxed grains in the opposite direction of heat flow. As a result of growth anisotropy, <001> is known as a preferred growth direction in cubic metals. So, dendrites which are well-aligned to heat flow direction grow easier [5,7]. Therefore, as a result of competitive growth mechanism in the starter block, a texture close to <001> is formed due to blocking of misaligned dendrites and branching of the secondary dendrite arms of well-aligned dendrites[5, 11].

A continuous distribution of active nucleation sites over the chill plate has been explained using a Gaussian distribution as a function of undercooling (ΔT), as describe below Eq. (1) [15]:

$$n_{(\Delta T)} = \int_0^{\Delta T} \frac{dn}{d(\Delta \acute{T})} d(\Delta \acute{T}) \qquad \text{Eq. (1)}$$

In the later equation, distribution of nucleation sites, dn/d(ΔT), describes the grain density increase, d*n*, which influenced by an increase in the undercooling d(ΔT). Therefore, density of active nucleation sites at a given undercooling, $n_{(\Delta T)}$, can be given by the integration of the distribution above.

For simplicity, the model is described in 2-dimensions as schematically depicted in **Error! Reference source not found.**. In two dimensions, we suppose that $n_{(\Delta T)}$ is the linear grain density on the surface of the chill. So the number of nucleation sites at a given undercooling is given by integration of the Eq. 1 from zero to the given undercooling. Undercooling on the chill is induced by the melt/chill interface heat transfer coefficient (IHTC).

Therefore, initial number of grains on the chill surface is influenced by IHTC which is induced by the water flow rate in the cooling system.

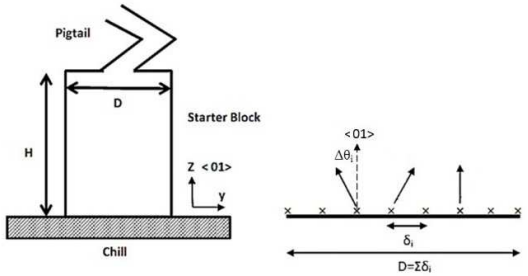

Fig. 1. Schematic Illustration of the two Dimensional Analytical Model.

As shown in the **Error! Reference source not found.**., the distance between neighboring grains is defined as δ_i. For a uniform grain distribution over the chill, δ_i is related to the number of grains on the chill and in the case of a starter block with a diameter of D, it can be explained as Eq. (2):

$$\delta_i = \frac{D}{D.n_{(\Delta T)}} = \frac{1}{n_{(\Delta T)}} \qquad \text{Eq. (2)}$$

It can be concluded from Eq. 2 that the distance between chilled grains, δ_i, is reversely related to the nucleation undercooling.

As seen here, by increasing the undercooling, nucleation density will be increased and, therefore, based on Eq. 2, δ_i will be decreased.

After the nucleation of chilled grains, columnar grains will grow in the opposite direction of heat flux extraction from the melt.

As mentioned before, grains with preferred growth direction parallel to the heat flow direction will be more consistent. Because of the random nature of nucleation process, each grain has a random orientation with respect to the horizon. As a result of four-fold symmetry of dendritic structure, in 2-D, dendrite orientation with respect to the <01> direction varies between $-\pi/4$ and $\pi/4$.

Therefore, each grain has a deviation from <01> direction, defined as $\Delta\theta_i$ as schematically is shown in Fig. 1.

It is supposed that grain orientations vary by 1° in the range of $-\pi/4$ and $\pi/4$, and so, there exist ninety different orientations. So, the number of grains with misorientation less than $-\Delta\theta$ to $\Delta\theta$ with respect to <01> direction, can be estimated as a probable expression Eq. (3):

$$\frac{\Delta\theta}{90} n_{(\Delta T)} = n_{\Delta\theta\,(\Delta T)} \qquad \text{Eq. (3)}$$

At which, $n_{\Delta\theta(\Delta T)}$ is the linear grain density of nucleation sites which have a misorientation from preferred <01> direction lower than $\Delta\theta$. By the combination of Eq. 2 and Eq. 3, the distance between grains having a deviation from $-\Delta\theta$ to $\Delta\theta$ can be calculated using Eq. (4):

$$\delta_{i(\Delta\theta)} = \frac{1}{n_{\Delta\theta\,(\Delta T)}} = \frac{90}{\Delta\theta.n_{(\Delta T)}} \qquad \text{Eq. (4)}$$

In the case of two converging dendrites, Zhou et al. [5] reported that the primary trunk of well-aligned grain stops the growth of misaligned grain.

So, as shown in Fig. 2., the height at which misaligned dendrite will be blocked by a well-aligned dendrite, h, can be expected as Eq. (5):

$$h = \delta_i \tan\left(\frac{\pi}{2} - \Delta\theta\right) \qquad \text{Eq. (5)}$$

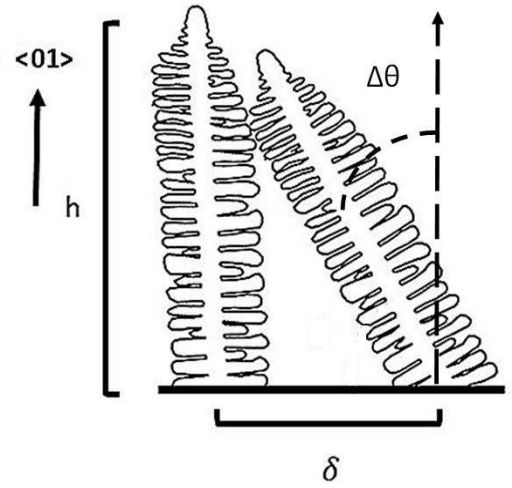

Fig. 2. Geometrical Situation of Two Converging Grains Used in the Analytical model.

In fact, h can be explained as the height at which dendrites with misorientation greater than Δθ have been overgrown by the well-aligned dendrites. In the starter block with a grain distribution density of $n_{(\Delta T)}$, this situation can be explained as below Eq. (6):

$$h_{\Delta\theta} \leq \frac{90}{\Delta\theta . n_{(\Delta T)}} \tan\left(\frac{\pi}{2} - \Delta\theta\right) \qquad \text{Eq. (6)}$$

As seen in the equation above, the height at which a texture with a deviation less than Δθ is formed, depends on two main parameters; the undercooling which affect the active nucleation site density, and the deviation angle, Δθ. As expected, the less deviation from <001> occurs at a higher height from the chill. Also the model describes that increasing the initial grain density, which means higher undercooling, would lower the height of preferred texture formation.

In the case of three dimensional competitive grain growth, growing dendrites are more constrained in comparison with two dimensional growth. Therefore, the height of texture formation may be equal to or lesser than the expression on the right hand side of Eq. 6.

2.2. Directional Solidification

To evaluate the present analytical model, experiments and numerical simulation using cellular automaton-finite element method (CAFE), was used. The directional solidification process was carried out using laboratory vertical Bridgman type furnace. Pure aluminum and copper (>99.9%) were melted in an alumina crucible in a resistance furnace to produce Al-3wt% Cu alloy. Then the melt were poured in a zircon mold which was mounted over the water cooled copper chill and heated up to 800˚C in the hot zone.

Heat extraction from the chill is controlled by the use of water flow rate in contact with copper chill as well as interface heat transfer coefficient between melt/chill.

Therefore, undercooling of the melt at the interface of the chill/melt depends on the heat extraction from the chill as well as heat input from the furnace.

To produce different nucleation undercooling, water flow rate was controlled in the cooling system.

Two different conditions were produced with different cooling rates, which produced different heat transfer coefficient.

To achieve a uniform temperature distribution in the melt as well as steady state condition, ceramic mold was held in the hot zone for 30 minutes before water cooling process starts and then it has been withdrawn from the hot zone at the constant rate of 3 mm/min. Increasing water flow rate increases undercooling of the melt in the chill/melt interface and according to Eq. 1, the nuclei density will be increased.

Variation of temperature at a point near the chill/melt interface was measured using a calibrated K-type thermocouples and the results were recorded using a data acquisition apparatus and thermal analysis system. Solidified samples then were cut, polished, and chemically etched with H_2O-HF solution to reveal the macro grain structure.

2.3. Numerical Simulation

2-D Cellular Automaton method was used for numerical simulation of the nucleation and growth process. Accuracy of cellular automaton calculations depends on the accurate determination of the temperature distribution in the domain during the process.

While heat extraction through melt/chill interface is dominated, interface heat transfer coefficient (IHTC) should be set to accurate value of numerical simulation. So, interface heat transfer coefficient of melt/chill interface was measured using thermal analysis followed by finite element inverse modeling. Because the contact situation of melt/chill interface varies by temperature, IHTC varies with temperature during cooling.

To calculate the variation of IHTC with temperature, thermal history of the melt was determined using a calibrated thermocouple. Then finite difference inverse calculations were used to determine the real IHTC. Variation of IHTC versus temperature is shown in Fig. 3. As it is shown, where perfect contact between melt and chill exists, IHTC value is high.

The IHTC were decreased gradually as a result of imperfect contact between solidified portion of the sample and chill. The same results were reported by other investigators. [14] IHTC for sample C1 is higher than that of C2 particularly at higher temperature, which the contact between melt and chill is perfect. It is due to higher water flow rate in the cooling system.

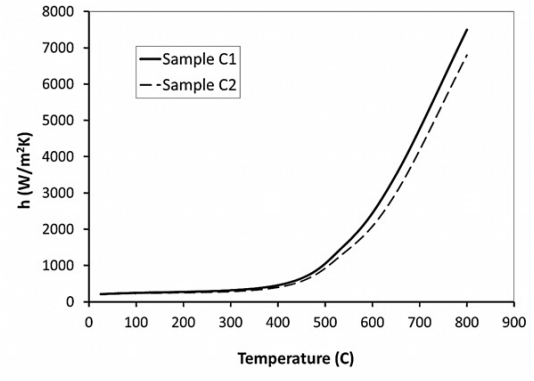

Fig. 3. Variation of interface heat transfer coefficient vs. temperature calculated from inverse modeling.

3. Results and Discussion

3.1. Cooling Curves

Variation of temperature versus time at a point in the starter block near the interface of the melt/chill is depicted in Fig. 4. for two specimens. As seen in this figure, to reach a steady state condition and uniform distribution of temperature in the melt, the sample is held in the furnace while there is no water flow in the chill. So, at the initial times of the process, the temperature is constant for two cases. At a point which is marked using a black arrow, water cooling is started. After the water cooling is started, the melt was undercooled at a high rate as a result of heat extracted from the water cooled chill with a high value of interface heat transfer coefficient between the chill and melt. As expected, as a result of higher heat transfer coefficient between chill and melt, especially at higher temperature, for the sample with the higher water flow rate (sample C1), the cooling rate is higher than the other.

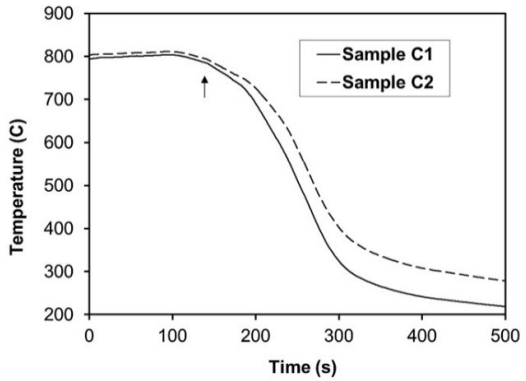

Fig. 4. Cooling curves for two samples C1 and C2 at a point near chill/melt interface; the arrow shows the start point of water flow in the chill.

The higher cooling rate of sample C1 at the beginning of the nucleation process will cause the melt to reach greater nucleation undercooling in comparison with sample C2. As seen in Fig. 4., at a constant time, the temperature for sample C1 is lower than sample C2. So, it can be concluded that undercooling increased by increment of the water flow rate in the chill. It is due to higher heat flux extracted from the melt at a higher water flow rate as a result of the higher IHTC for sample C1 (See Fig. 3.). Cooling rates in the range of the beginning and the end of nucleation process were determined to be 4 and 2.4 ˚C/s for samples C1 and C2, respectively. As supposed in the analytical model, for two cases described later, the effect of thermal gradient and isotherm velocity on the growth of dendrite was neglected. As shown in Fig. 3, at lower temperatures (below 500°C), interface heat transfer coefficient for the two cases are almost the same.

Therefore, as shown in Fig. 4., the slope of cooling curves for two cases are the same in this temperature range. It is because that, in this situation heat flow is mainly controlled by radiation in the cold chamber of the furnace and heat extraction from the chill is not dominated. It may be concluded that thermal gradient and isotherm velocity are almost same for two samples. So, the effect of thermal gradient and isotherm velocity on the dendritic growth and texture formation will be neglected to some extend.

Nucleation undercooling was calculated from the difference between nucleation point (T_N) and minimum nucleation temperature (T_{min}) determined from cooling curve and with the aim of the first derivative of temperature versus time. The nucleation point (T_N) is the temperature at which a great raise starts in the derivative curve. The position of nucleation point (T_N) and minimum nucleation temperature (T_{min}) is shown in Fig. 5.

The value of nucleation undercooling for Al-3wt%Cu alloy ($\Delta T_N=T_N-T_{min}$) is determined to be about 4˚C and 2.5 ˚C for sample C1 and C2, respectively.

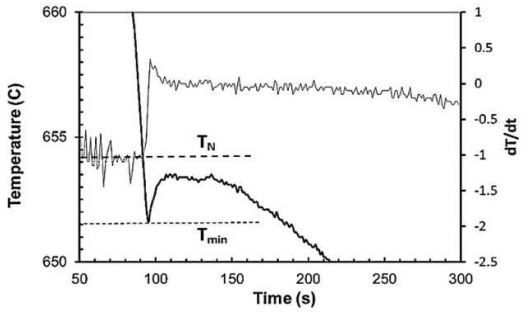

Fig. 5. Cooling curve and first derivative of temperature versus time in the range of 650 – 660 ˚C form Al-3wt%Cu alloy.

3.2. Grain Structure of Solidified Sample

Optical micrographs were studied to evaluate the effect of undercooling on the solidified structure of the starter block. The grain structure of the starter block at the longitudinal cross section is illustrated in Fig. 6. As shown in this figure, for sample C1, the

initial grain number at the bottom of the starter block is higher that sample C2. As mentioned previously, it is due to the higher cooling rate for sample C1. The higher cooling rate for sample C1 caused finer columnar grains which means lower distance between neighboring dendrites such as schematically shown in Fig. 1.

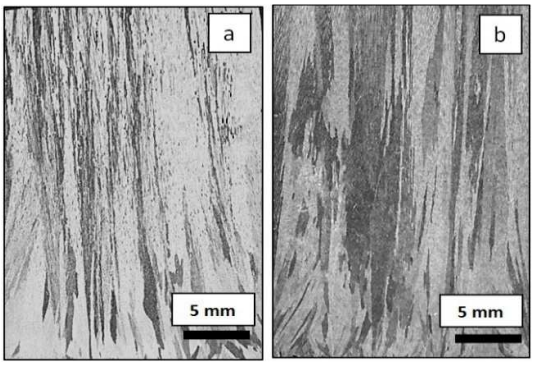

Fig. 6. Grain structure of the starter block in longitudinal cross section. a) Sample C1: 4 ˚C/s b) Sample C2: 2.4 ˚C/s.

3.3. CAFE Simulation

Cellular automaton-finite element (CAFE) method was used to verify the calculation results of the analytical model described in the previous section. Two different situations for samples C1 and C2 have been developed as described previously. The simulated grain structure of the samples is shown in Fig. 7. Simulated grain structure of the starter block is the same as the structure of the experimentally solidified samples shown in Fig. 6.

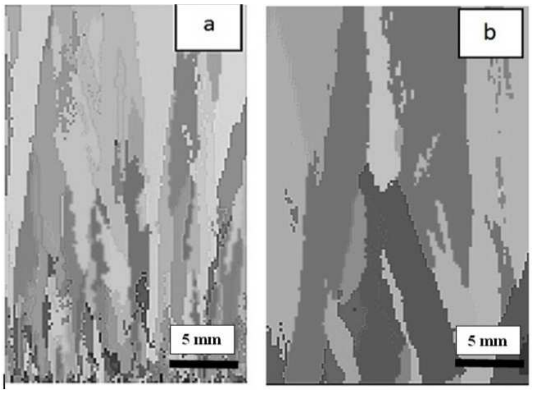

Fig. 7. Simulated grain structure of the starter block. a) C1: 4 ˚C/s b) C2: 2.4 ˚C/s.

Variation of simulated grain misorientation from <01> direction and grain densities are shown in Fig. 8. and Fig. 9., respectively. It is important to note that numerical and experimental results are in a good agreement with analytical model. As seen in Fig. 8, increasing the undercooling decreases the misorientation from <01> direction. Based on the analytical model, increasing the nucleation undercooling increases the grain density and therefore the distance between the grains will be decreased. Based on Eq. 6, the height at which grains with preferred orientation grow over the non-preferred ones, will be decreased. It should be mentioned that, the height of preferred texture formation has been increased for sample with lower cooling rate as a result of lower initial nucleation sites.

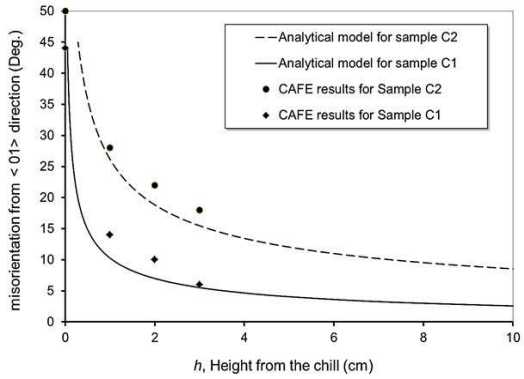

Fig. 8. Comparison between CAFE simulation results and calculation of the present model for samples C1 and C2.

The number of grains will be decreased by increasing the height from the chill as a result of competitive growth mechanism (Fig. 9.). At the beginning of the process, grain density decreases faster in the case of higher cooling rate (sample C1). In this case, undercooling on the chill plate is higher and, therefore, the number of grains at chill/melt interface will be increased. So, according to Eq. 2, the distance between initial grains, δ_i, decreases. Therefore, based on the Eq. 5 misaligned grains will be overgrown by the well-aligned and suppressed at a lower height from the chill.

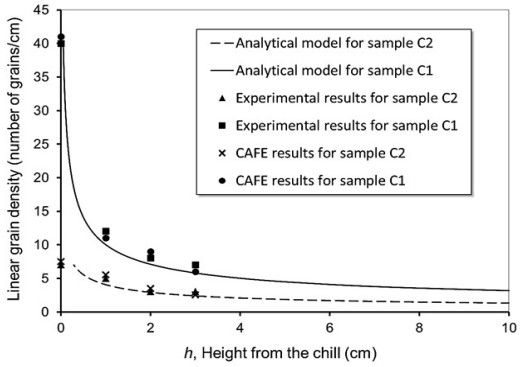

Fig. 9. Comparison between model calculations, numerical simulation and experimental results for variation of linear grain densities versus height from the chill.

4. Conclusions

Based on this investigation, conclusions can be followed as:

1. A simple analytical model is derived from the physical concept of competitive grain growth in a starter block. It determines the effect of nucleation undercooling on the texture formation and verified by the experimental and CAFE simulation results.
2. The model described that the height of <01> texture formation during directional solidification depends on the nucleation undercooling, and therefore, nucleation sites as well as the deviation of the grains from <01> direction.
3. Based on the simple analytical model, it can be concluded that the preferred texture formation and decrement of grain density will be encouraged by the increment of initial nucleation sites caused by nucleation undercooling.

References

[1] A. Wagner, B. A. Shollock and M. McLean, Mater. Sci. Eng. A, (374)2004, 270.
[2] X. Zhao, L. Liu, Zh. Yu, W. Zhang and H. Fu, Mater. Charact., (61)2010, 7.
[3] Q. Dong, J. Shen and X. Yue, Mater. Lett., (228)2018, 281.
[4] B. X. Xu, X. M. Wang, B. Zhao and Z. F. Yue, Mater. Sci. Eng. A, (478)2008, 187.
[5] Y. Z. Zhou, A. Volek and N. R. Green, Acta. Mater., (56)2008, 2631.
[6] N. Siredey, M. Boufoussi, S. Denis and J. Lacaze, J. Cryst. Growth., (130)1993, 132.
[7] Zh. Wang, J. Li and J. Wang, J. Cryst. Growth., (328)2001, 108.
[8] N. Wang, L. Liu, X. Zhao, T. Huang and J. Zhang, J. Alloys Compd., (586)2014, 220.
[9] X. H. Zhan, Z. B. Dong, Y. H. Wei and R. Ma, J. Cryst. Growth., (311)2009, 4778.
[10] P. Carter, C. A. Gandin and R. C. Reed, Mater. Sci. Eng. A, (280)2000, 233.
[11] J. Li, Z. Wang, Y. Wang and J. Wang, Acta. Mater., (60)2012, 1478.
[12] M. Rappaz and Ch. A. Gandin, Acta metall. Mater., (41)1993, 345.
[13] X. Meng, J. L. Tao Jin, X. Sun, Ch. Sun and Zh. Hu, J. Mater. Sci. Technol., (27)2001, 118.
[14] L. Ying, L. Baicheng, Tsinghua Sci. Technol., (11)2006, 495.
[15] J. A. Dantzig, M. Rappaz, Solidification, EPFL press, Switzerland, 2008.
[16] Y. Dong, K. Bu, Y. Dou and D. Zhang, J. Mater. Process. Technol., (211)2011, 2123.